



INTERNATIONAL ATOMIC ENERGY AGENCY  
UNITED NATIONS EDUCATIONAL, SCIENTIFIC AND CULTURAL ORGANIZATION  
**INTERNATIONAL CENTRE FOR THEORETICAL PHYSICS**  
I.C.T.P., P.O. BOX 586, 34100 TRIESTE, ITALY, CABLE CENTRATOM TRIESTE



**SMR.764 - 2**

RESEARCH WORKSHOP ON CONDENSED MATTER PHYSICS  
13 JUNE - 19 AUGUST 1994

**WORKING GROUP ON  
"DISORDERED ALLOYS"  
8 - 19 AUGUST 1994**

---

*"An augmented space recursive technique  
for the calculation of electronic structure  
of random binary alloys"*

*Part I*

**Abhijit MOOKERJEE  
S.N. Bose National Centre for Basic Sciences  
DB17, Sector 1, Salt Lake City  
Calcutta 700064  
INDIA**

---

*These are preliminary lecture notes, intended only for distribution to participants*

LECTURE 1

# AN AUGMENTED SPACE RECURSIVE TECHNIQUE FOR THE CALCULATION OF ELECTRONIC STRUCTURE OF RANDOM BINARY ALLOYS

**ABHIJIT MOOKERJEE\***

S. N. Bose National Centre for Basic Sciences,  
DB 17, Sector 1, Salt Lake City, Calcutta 700064, INDIA

9 August, 1994

### Abstract

In this lecture we shall present a computationally feasible and fast technique for obtaining the electronic structure of random alloys which allows us to incorporate effects like clustering, short-ranged order and off-diagonal disorder arising out of size mismatch and consequent lattice distortions. The method combines the Augmented Space Technique with the recursion method and the tight-binding LMTO. AgPd, CuZn, CuPd and FeTi alloys are studied to illustrate our procedure.

---

\*The work reported here was done in collaboration with Indra Dasgupta and Tanusri Saha. Our programme package included the LMTO package from O.K. Andersen and his group at Stuttgart, the Cambridge Recursion Package developed by Chris Nex and parts of the TB-LMTO programme of Patricio Vargas

## 1 INTRODUCTION.

The first principles description of the electronic structure and properties of disordered transition metal alloys is a challenging problem. The absence of translational symmetry is the main obstacle in the construction of a quantitative theory comparable in accuracy and efficiency with those for crystalline solids, based on the Bloch theorem and standard band structure methods. The electronic structure and properties of transition metal alloys are believed to be governed mainly by the relatively localized d-electrons. Hence it was customary to use semi-empirical tight-binding Hamiltonians to describe their electronic properties. In spite of encouraging successes the electronic structure calculation based on the semi-empirical tight-binding Hamiltonians have some underlying approximations which are often unjustified [1].

The main step towards constructing first principles tight-binding Hamiltonians began with the tight-binding linearized muffin tin orbital method (TB-LMTO) proposed by Andersen and Jepsen [2]. In the TB-LMTO the Hamiltonian is parametrized by a set of potential parameters (to be discussed later in the text) which are derived selfconsistently from a first principles theory and are not empirical.

The other central issue for a first principles calculation is the construction of realistic structural models. In principle, the structure can be varied in parallel to the calculation of electronic structure. This has been reformulated in terms of classical Lagrangian dynamics by Car and Parinello [3]. This method has been extensively used in ab initio molecular dynamics simulations of liquid and amorphous Si and other s-p bonded systems, but the underlying pseudopotential method makes its application to systems with transition metals impractical. Recently there have been attempts at ab initio molecular dynamics based on the full potential LMTO method. Methfessel and Schilfgaarde [4] have derived an accurate force theorem, quite distinct from Hellman-Feynman theorem. They have implemented a Car Parinello type of dynamics in a new full potential LMTO, which is suitable for arbitrary geometries, and calculated the properties of small Ag clusters. Though first principles electronic structure calculations for topologically dis-

ordered systems demand realistic structural models, but for substitutionally disordered transition metal alloys, calculations in the framework of TB-LMTO is regarded to be first principles.

Kudrnovský and Drchal [5] have demonstrated that the coherent potential approximation (CPA) based on the linearized version of the screened KKR (TB-LMTO) accurately describes the electronic structure of random alloys (both metallic and semiconducting) and disordered surfaces in a large class of alloy systems. Within the TB-LMTO method full charge self-consistency can be achieved and is usually carried out for elements, compounds and ordered alloys. Kudrnovský *et.al.* [6] has demonstrated that the flexibility in the choice of Wigner-Seitz radii in random binary alloys makes possible approximate, yet accurate and consistent, treatment of charge self-consistency without going through the full charge self-consistency cycles. The self consistency involved in the solution of the CPA equation is not trivial and one has to invoke subtle mathematical procedures to ensure proper convergence. Recently Singh and Gonis [7] have criticized the TBLMTO-CPA proposed by Kudrnovský and Drchal on the grounds that ensemble or configuration averaging involved in their method did not properly take into account the multi-site nature of the TB-LMTO basis functions resulting in an inconsistency in the configuration averaged Green function. Although these authors try to circumvent this difficulty by making a pure L approximation for the site diagonal linearized muffin tin orbitals (LMTO's), the fact remain that by their very nature, the TB-LMTO formalism involves multisite summations.

Formally the APW [8] and the KKR [9], the parent methods of the LPAW [10] and the LMTO [11] respectively, involve very few uncontrolled approximations and are therefore expected to be superior in accuracy and reliability than their linearized versions. However, the non-linear secular equations involved are computationally costly. Extensions of these methods to disordered systems further emphasizes computational difficulties. Of the mean field approaches, the single site CPA has been successfully implemented within these frameworks [12]. Certainly, where the single site approximation is valid, the APW

or KKR-CPA are the most accurate and reliable methods. However, there are many situations where such single site approximations begin to fail: as in cases where clustering effects become important [13] (*e.g.* in the impurity bands of split band alloys, like the Zn-band in Cu-rich CuZn alloys), where short ranged order dominates leading to ordering or segregation [14], where local lattice distortions because of size mismatch of the constituents leads to essential off-diagonal disorder in the structure matrix  $S_{RL,R'L'}$  [15] (as in CuPd or CuBe alloys) or where topological disorder of the underlying lattice makes the structure matrix depend on the specific pair of sites  $\{R,R'\}$  [16] (as in glassy materials like FeB). In such situations, the generalization of the CPA is not a trivial problem [13]. The embedded cluster method (ECM) [17] where a cluster, in all its various disordered configurations, is embedded in a CPA medium is not self-consistent in the spirit of coherent potential approximations. The molecular CPA [18] breaks the translational symmetry of the averaged medium and the artificial zone boundary effects introduced cannot be controlled. Of the cluster generalizations, only two retain herglotz analytic properties: the Travelling Cluster Approximation (TCA) [19] and the Cluster CPA (CCPA) [20], both based on the Augmented Space formalism (ASF) [21] which is also the basis of the work presented here. The computational intractability of both these methods whenever the size of the cluster becomes even reasonably large is clearly perceived if we refer to [19, 20]. To date, calculations on the KKR based CCPA have been successfully carried out only on pair clusters [22].

This provides a motivation to look for alternative approaches for the generalization of the single site approximation. The TB-LMTO method is a likely framework. The purpose of this communication is to propose and implement a method which is based on the Augmented Space Formalism (ASF) [21] introduced by one of us, coupled with the recursion method of Haydock, Heine and Kelly [23]. This method retains the herglotz properties of the configuration averaged Green function. The coupling to the recursion method allows effects of quite large clusters to be taken into account. Since the recursion method is intrinsically multisite, off-diagonal disorder and the multisite nature of the LMTO's is

not a problem. We shall demonstrate that the use of local point group symmetries of the underlying lattice and the larger symmetries in the full augmented space arising out of homogeneity of disorder allows us to work on an irreducible subspace of the augmented space with vastly reduced rank and makes the method tractable even on small desktop workstations.

The paper is organized as follows : in section 2 we briefly review the TB-LMTO method required for the purpose of augmented recursion. In section 3 we discuss the real space recursion for calculating the Green function, with an emphasis on the symmetry properties which can be exploited to reduce the work-load of computation. In section 4 we briefly discuss the augmented space theorem for the calculation of configuration average of any function of random variables. Section 5 is devoted to the detailed discussion of the augmented space recursion method of calculating the configuration averaged Green function. Section 6 deals with computational details. In section 7 we discuss our results on fcc based AgPd and CuPd alloys and bcc based FeTi and CuZn alloys. Conclusion and additional comments regarding the further refinement of our method is given in section 8.

## 2 THE ELECTRONIC STRUCTURE CALCULATIONS WITH THE TIGHT-BINDING LMTO.

In the LMTO method, an energy independent basis set  $\chi_{RL}(\tau_R)$  is derived from the energy dependent partial waves in the form of the muffin tin orbitals (MTO). The set is constructed in such a way that it has the following characteristics: (a) it is appropriate to the one electron effective potential  $V(r)$  of the solid, (b) it is a minimal basis set and (c) it is continuous and singly differentiable in all space. In this section we will restrict ourselves to the most tight-binding representation of the LMTO, resulting in a sparse Hamiltonian, required for the purpose of augmented space recursion.

As a first step in the LMTO method, the space is partitioned into two regions viz. the muffin tin spheres centered at various atomic (if necessary, also interstitial) sites  $R$  and the interstitial region. In the atomic sphere approximation (ASA) the touching muffin tin

spheres are substituted by overlapping Wigner-Seitz spheres, thereby dispensing with the interstitial component. It has been argued that if the overlap between the Wigner-Seitz spheres is less than 30% then ASA is a good approximation and gives reliable results [24].

In the most tight-binding representation, a LMTO basis orbital of collective angular momenta index  $L=(\ell m)$  centered at site  $R$ , is given in the ASA, by the expression:

$$\chi_{RL}^{\alpha}(\tau_R) = \phi_{RL}(\tau_R) + \sum_{R'L'} \dot{\phi}_{R'L'}^{\alpha} h_{RL,R'L'}^{\alpha} \quad (1)$$

$\tau_R = r-R$ . The function  $\phi_{RL}$  is the solution of the wave-equation inside the sphere of radius  $S_R$  at  $R$  for some reference energy  $E_{\nu RL}$  and is normalized within the sphere. The potential inside the sphere is calculated using the local density functional approximation (LDA). The radial part of the  $\dot{\phi}_{RL}^{\alpha}$  is related to the energy derivative of  $\phi_{RL}^{\alpha}(\tau_R)$  at the reference energy :

$$\dot{\phi}_{RL}^{\alpha}(\tau_R) = \dot{\phi}_{RL}(\tau_R) + \phi_{RL}(\tau_R) \phi_{RL}^{\alpha} \quad (2)$$

The quantity  $\phi_{RL}^{\alpha} = \langle \phi_{RL} | \dot{\phi}_{RL}^{\alpha} \rangle$  is the overlap. The expansion coefficients  $h_{\alpha}$  in equation (1) are given by

$$h_{RL,R'L'}^{\alpha} = (C_{RL}^{\alpha} - E_{\nu RL}) \delta_{RR'} \delta_{LL'} + (\Delta_{RL}^{\alpha})^{1/2} S_{RL,R'L'}^{\alpha} (\Delta_{RL}^{\alpha})^{1/2} \quad (3)$$

where  $C_{RL}^{\alpha}$  and  $\Delta_{RL}^{\alpha}$  are the potential parameters to be obtained from the potential function  $P^{\alpha}$  at the reference energy  $E_{\nu RL}$ .  $S_{RL,R'L'}^{\alpha}$  is the screened structure matrix whose elements in the most tight-binding representation are essentially zero beyond the second shell of neighbours in all closed packed structures. The screened structure matrix  $S^{\alpha}$  can be obtained from the canonical structure matrix  $S^0$  by the unitary transformation :

$$S^{\alpha} = S^0 (1 - Q^{\alpha} S^0)^{-1} \quad (4)$$

The set of parameters (screening constants)  $Q^{\alpha}$  which defines the above transformation are unique for all closely packed structures, and yields most localized structure constant with exponential decay rather than the usual power law behaviour.

There are several features of TB-LMTO orbitals, which make them distinct from atomic and atomic like orbitals used in the ordinary TB-calculations. The summation over the composite angular momentum index in equation (1) suggests that the TB-LMTO orbitals do not preserve pure L character. Further in equation (1)  $\phi_{RL}^{\alpha}(r_R)$  and  $\phi_{RL}^{\beta}$  are truncated outside the Wigner-Seitz sphere and the expansion coefficients vanish beyond the second shell of neighbours in all closed packed structures, so that all TB-LMTO orbitals are short-ranged, resulting in a sparse Hamiltonian in this representation. This is ideal for real space calculations based on the recursion method. The Hamiltonian and the overlap matrices for this basis are given by (with neglect of small terms) :

$$H = h + hoh + (I + ho)E_{\nu}(I + oh) \quad (5)$$

$$o = \langle \chi | \chi \rangle = (I + ho)(I + ho) \quad (6)$$

In equations ( 5) and ( 6) the summation indices RL, are suppressed for convenience. The matrix o is diagonal in RL representation and its value is determined by the logarithmic derivative of the function  $\phi$  at the sphere boundary. The Löwdin orthonormalized Hamiltonian in the ASA is given by:

$$H^{(2)} = E_{\nu} + h - hoh + hohoh - \dots \quad (7)$$

and the first order hamiltonian is given by

$$H^{(1)} = E_{\nu} + h \quad (8)$$

In equation ( 7) the parameter o determines the degree of non-orthogonality of the basis. Again  $o^{-1}$  has the dimension of energy and provides a measure of the energy window about the reference energy  $E_{\nu}$  for which the density of states obtained with  $H^{(1)}$  are reliable.

In order to perform a recursion calculation, we have to truncate the series given by equation (7) for computational tractability. This in turn introduces non-orthogonality of

the basis, so one has to make a compromise between the two for reliable results. The recursion involves repeated operation on the recursive basis by  $H^{(2)}$ . Since h is sparse, there is, in principle, no additional difficulty (other than enhanced computational time) in going beyond the first order hamiltonian. Recursion with  $H^{(1)}$  gives a Green function accurate to first order in  $(E - E_{\nu})$  [24]. The second term hoh is necessary for systems with wide bands specially for s-p states. We have used first order Hamiltonian in our subsequent calculation.

### 3 THE REAL SPACE RECURSION METHOD.

The real space recursion method, provides an efficient algorithm for the calculation of the resolvent  $(zI - H)^{-1}$  of a sparse Hamiltonian. In this section we will review the recursion method and demonstrate how the symmetry of the Hamiltonian can be exploited to reduce the work-load considerably. The method starts with a given vector,  $|u_0\rangle$ , and recursively generates a new set of vectors  $|u_i\rangle$ , which are constructed so as to be mutually orthogonal :

$$H|u_n\rangle = a_n|u_n\rangle + b_{n+1}|u_{n+1}\rangle + b_n|u_{n-1}\rangle \quad (9)$$

$$b_0^2 = \langle u_0 | u_0 \rangle$$

$$a_n = \langle u_n | H | u_n \rangle$$

the recursion coefficients  $a_n$  and  $b_n$  are the diagonal and off-diagonal elements of the tridiagonal Hamiltonian matrix in the new representation. The method also yields an explicit continued fraction form for the diagonal elements of the resolvent (the Green function):

$$\langle u_0 | (zI - H)^{-1} | u_0 \rangle = \frac{b_0^2}{E - a_1 - \frac{b_1^2}{E - a_2 - \dots}} \quad (10)$$

In practice the continued fraction is evaluated to a finite number of steps . Haydock [25] has mapped the contributions of the continued fraction coefficients to self-avoiding walks on the underlying space. He has shown that the dominant contribution comes from the walks that wind round the initial starting state . This allows one to work only on the finite part of the hilbert space: a particular sized cluster around the initial starting state . The continued fraction is complemented after a finite number of steps  $N$  with a suitable terminator. The terminator reflects the asymptotic properties of the continued fraction expansion of the resolvent accurately. Several terminators are available in the literature and we have chosen to use the terminator of Lucini and Nex [26]. The advantage of such a termination procedure is that the approximate resolvent retains the herglotz properties. It preserves the first  $2(N-2)$  moments of the density of states exactly. This represents the effect of a cluster at a distance  $(N-2)$  from the starting state. It also maintains the correct band-widths , band weights and the correct singularity of the band edges. It is worth mentioning that, for a tight-binding Hamiltonian, the recursion method has a work-load proportional to the size of the system rather than the cubic proportionality of the usual band structure super-cell methods, where the self-consistency is achieved at one k-point.

The work-load of the recursion can be further reduced if one exploits the symmetry of the Hamiltonian. The Hamiltonian described by (7) contains the information of both, the structure of the underlying lattice and the symmetry of the orbitals. It has been shown by Gallagher [27] that if the starting state of the recursion belongs to an irreducible representation of the Hamiltonian, then the states generated in the process of recursion belong to the same row of the same irreducible representation of the Hamiltonian. Further the recursion with the starting state corresponding to the different rows of the same irreducible representation are similar. The states belonging to the different irreducible representations or different rows of the same irreducible representation do not mix. So we need to retain only those states for the purpose of recursion and get the same resolution as with all of them. The recursion is done only with those states which are not related to one another by the point group symmetry of the underlying lattice. Once these state

vectors are identified, the recursion can be performed in the reduced space , modified with weight factors. Thus in the computation we need far less storage and time because the dimensionality of the matrix  $H$  is reduced drastically. In practice a starting site is chosen. The number of distinct equivalent sites , related to the starting site by the local point group symmetry, constitutes the weight of the starting site. As discussed earlier , in the process of recursion, these equivalent sites are not considered, and the calculation is confined only to the nonequivalent sites. For example for s-state hamiltonian on a lattice with cubic symmetry, all the non-equivalent sites are confined to  $(1/48)^{th}$  of the entire lattice . Inclusion of p orbitals, introduces preferred x , y or z directions and breaks the symmetry between x , y and z axis. Thus the point group symmetry operations which interchange between x , y and z co-ordinates are prohibited . Hence the irreducible part of the lattice instead of being  $(1/48)^{th}$  of the entire lattice now becomes  $(1/8)^{th}$ . If with each site  $R$  we attach weight  $W_R$  , which is given by the number of basis states equivalent to  $|R\rangle$  , then the whole process can be summarized as follows : In the new TB-LMTO reduced basis we have

$$\langle R, L | H | R, L \rangle = C_{R,L}^{\circ} \quad (11)$$

$$\langle R', L' | H | R, L \rangle = \sqrt{(W_R/W_{R'})} (\Delta_{R'L'}^{\circ})^{1/2} S_{R',L',R,L}^{\circ} (\Delta_{R,L}^{\circ})^{1/2} \beta_R(L, L') \quad (12)$$

where  $R$  and  $R'$  both belong to the irreducible part of the lattice.  $\beta_R(L, L')$  is the factor which can be either 0 or 1 , depending on whether the position occupied by the site  $R$  is a symmetry position with respect to orbitals  $L$  and  $L'$  or not . This fact can be made more transparent in the following way : the structure matrix element connecting two orbitals occupying the two different sites is given by the two-centre Slater-Koster integrals . Apart from a factor made of  $\pi$  and  $\sigma$  integrals the Slater-Koster integral contains a factor made up of direction cosines of the vector joining the two basis states between which the matrix element is taken . It reflects the symmetry property of the overlapping orbitals . Now for the different equivalent sites connected to a given site , this direction cosine has different signs . In the effective irreducible basis , which is a linear combination of the old basis,

a particular linear combination may give rise to a zero Hamiltonian matrix element . We shall call these positions, where such zero matrix element occur, the symmetry positions with respect to orbitals L and L'. The representation of the Hamiltonian in terms of the irreducible basis sets reduces the rank of the Hamiltonian matrix. The workload of the recursion reduces drastically . Such a reduction is absolutely necessary for the purpose of augmented space recursion to be discussed in the subsequent section.

## 4 AUGMENTED SPACE FORMALISM.

The augmented space formalism enables one to deal with the problem of averaging over disorder configurations. The formalism puts configuration averaging on the same footing as quantum mechanical averaging by augmenting the hilbert space spanned by the wave-functions with a disorder or configuration space spanned by the different realizations of the random Hamiltonian. The method of configuration averaging by the augmented space theorem has been discussed earlier [21], and we shall restrict ourselves only to the salient features of the method.

Let us suppose that the Hamiltonian describing a system is characterized by a set of independent random variables  $\{ x_i \}$  The probability density of  $\{ x_i \}$  is assumed to have a finite moments to all orders so that we may write :

$$p(x_i) = -\frac{1}{\pi} \text{Im} \langle f_0^i | (x_i + i0)I - M^{(i)} \rangle^{-1} | f_0^i \rangle \quad (13)$$

where  $M^{(i)}$  is an operator on the space  $\phi_0^i$  of rank N, spanned by the N possible configurations of  $x_i$  ;  $| f_0^i \rangle$  is the configuration *ground state*. A suitable choice of the basis is one that makes  $M^{(i)}$  tridiagonal. This tridiagonal representation may be immediately obtained by looking at the continued fraction expansion for  $p(x_i)$  :

$$p(x_i) = -\frac{1}{\pi} \text{Im} \frac{1}{x_i - a_i - \frac{b_i^2}{\dots}} \quad (14)$$

Since  $p(x_i) > 0$  and has finite moments to all orders, it always has a convergent continued fraction expansion with real coefficients  $\{ a_n, b_n \}$  . The representation of  $M^{(i)}$  has

$a_i$  down the diagonal and  $b_i$  down the off-diagonal positions. For a random binary alloy  $A_x B_{1-x}$  ,  $p_i(n_i)$  may be written as:

$$p_i(n_i) = x\delta(n_i - 1) + (1 - x)\delta(n_i) \quad (15)$$

where

$$n_i = \begin{cases} 1, & \text{for } i = A \\ 0, & \text{for } i = B \end{cases}$$

It immediately follows then  $p_i(n_i)$  satisfies the required conditions namely

$$\int p_i(n_i) n_i^m dn_i = \text{finite}$$

for all m and

$$p_i(n_i) \geq 0$$

For this  $p_i(n_i)$ ,  $M^{(i)}$  is a tridiagonal matrix in a space  $\phi_i$  of rank 2 spanned by  $|f_0^i\rangle$  and  $|f_1^i\rangle$  with a representation

$$M^{(i)} = \begin{pmatrix} x & \sqrt{x(1-x)} \\ \sqrt{x(1-x)} & (1-x) \end{pmatrix}$$

in this basis.

The formalism now states that the configuration average over any function H  $\{ x_i \}$  , may be written as:

$$\int P(\{ x_i \}) H \{ x_i \} d \{ x_i \} = \langle f | \tilde{H} | f \rangle \quad (16)$$

where  $\tilde{H}$  is the same functional operator of  $\{ M^{(i)} \}$  as H was a function  $\{ x_i \}$  and  $|f\rangle = \prod_i |f_0^i\rangle$  is the configuration *ground state* . Configuration averaging has been reduced to the problem of the *ground state* matrix element in the augmented space – an idea familiar in quantum mechanical averaging.

## 5 AUGMENTED SPACE RECURSION .

It is clear from the discussion in the preceding two sections that , for a system described by a disordered Hamiltonian , the recursion method defined on the augmented space enables one to calculate the configuration averaged Green function directly. The advantage of the method is that it does not involve a single site approximation or the solution of any self-consistent equation as required in the CPA or its generalizations. Further one can treat both diagonal and off-diagonal disorder on an equal footing. In spite of its immense potential the method could not be used for practical calculations because of the large dimension of the augmented space :  $N \times 2^N$  for a system with N sites and disorder characterized by a binary probability distribution. However, in analogy to real space symmetry , if we exploit the symmetry of the augmented space which arises due to homogeneity of disorder, then the rank of the augmented space is reduced and the augmented space recursion becomes tractable .

The starting point for the augmented space recursion , is the most localized sparse tight-binding Hamiltonian derived systematically from the LMTO-ASA theory and generalized to substitutionally disordered random binary alloys :

$$H_{RL,R'L'}^{\circ} = \hat{C}_{RL} \delta_{RR'} \delta_{LL'} + \hat{\Delta}_{RL} S_{RL,R'L'}^{\circ} \hat{\Delta}_{R'L'} \quad (17)$$

$$\hat{C}_{RL} = C_{RL}^A n_R + C_{RL}^B (1 - n_R) \quad (18)$$

$$\hat{\Delta}_{RL} = \Delta_{RL}^A n_R + \Delta_{RL}^B (1 - n_R) \quad (19)$$

Here R denotes the lattice sites and L=( $\ell$  m) are the orbital indices (for transition metal  $\ell < 2$ )  $C_{RL}^A$ ,  $C_{RL}^B$  and  $\Delta_{RL}^A$ ,  $\Delta_{RL}^B$  are the potential parameters of the constituents A and B of the alloy.  $n_R$  are the local site occupation variables which randomly take values 1 and 0 according to whether the site is occupied by an A atom or not. From the discussion in section 4. , it is clear that the representation of the Hamiltonian in the augmented

space  $\tilde{H}$  consists of replacing the local site occupation variables  $\{ n_R \}$  by  $\{ M^R \}$ , and is given by:

$$\begin{aligned} \tilde{H} = & \sum_{RL} (C_{RL}^B \tilde{I} + \delta C_{RL} \tilde{M}^R) \otimes a_R^\dagger a_R + \dots \\ & + \sum_{RL} \sum_{R'L'} (\Delta_{RL}^B \tilde{I} + \delta \Delta_{RL} \tilde{M}^R) S_{RL,R'L'}^{\circ} (\Delta_{R'L'}^B \tilde{I} + \delta \Delta_{R'L'} \tilde{M}^{R'}) \otimes a_{R'}^\dagger a_{R'} \end{aligned}$$

where,

$$\delta C_{RL} = (C_{RL}^A - C_{RL}^B)$$

$$\delta \Delta_{RL} = (\Delta_{RL}^A - \Delta_{RL}^B)$$

Other parameters have their usual meaning and  $\tilde{I}$  is the identity operator defined in the augmented space .  $\tilde{M}^R$  in the second quantized notation is given by:

$$\tilde{M}^R = x b_{R0}^\dagger b_{R0} + (1-x) b_{R0}^\dagger b_{R0} + \sqrt{x(1-x)} (b_{R0}^\dagger b_{R1} + b_{R1}^\dagger b_{R0}) \quad (20)$$

$(b_{R0}^\dagger, b_{R0})$  and  $(b_{R1}^\dagger, b_{R1})$  are the creation and annihilation operators in the augmented space , where each site is characterized by two states ( 0,1 ), which may be identified with the up and down states of an Ising system . The configuration states are stored extremely efficiently in bits of words and the algebra of the Hamiltonian in the configuration space mirrors the multi-spin coding techniques used in numerical works with the Ising model .

The Hamiltonian is now an operator in a much enlarged space  $\Phi = H \otimes \prod \phi^R$  (the augmented space), where H is the *real space* spanned by the countable basis set  $\{|R\rangle\}$  . The enlarged Hamiltonian does not involve any random variables but incorporates within itself the full information about the random occupation variables . If we substitute eq (22 ) for  $M^R$  , then with the aid of little algebra we can show that the augmented space Hamiltonian contains operators of the following types as discussed in [28].

(a)  $a_R^\dagger a_{R'}$  with  $R=R'$  and  $R \neq R'$  terms . The operators acting on a vector in the augmented space changes only the real space label , but keeps the configuration part

unchanged.

(b)  $a_R^\dagger a_{R'} b_{k\lambda}^\dagger b_{k\mu}$  with  $R = R'$  and  $R \neq R'$  terms .  $k$  is  $R$  or  $R'$  ,while,  $\lambda$  and  $\mu$  may take value 0 and 1 . These operators acting on an augmented space vector may change the real space label ( if  $R \neq R'$  ) . In addition , they may also change the configuration at the site  $R$  or  $R'$  (if  $\lambda \neq \mu$ ). This resembles a single spin flip Ising operator in configuration space .

(c)  $a_R^\dagger a_{R'} b_{R\lambda}^\dagger b_{R\mu} b_{R'\nu}^\dagger b_{R'\xi}$  with  $\lambda, \mu, \nu, \xi$  taking values 0 and 1. The operators may change the real space label ( if  $R \neq R'$  ) , as well as the configuration either at  $R$  or  $R'$  or both. This resembles a double spin flip Ising operator in the configuration space .

A basis  $|m\rangle$  in the hilbert space  $H$  is represented by a column vector  $C_m$  with zeros everywhere except at the  $m$ -th position . The inner products are defined as

$$\langle m | \odot | n \rangle = C_m^T C_n$$

$$a_m^\dagger a_n C_p = \delta_{np} C_m$$

A member of the basis in  $\prod^{\otimes} \phi_R$  has the form

$$|f_{\lambda_1}^1 \otimes f_{\lambda_2}^2 \otimes \dots\rangle$$

where each  $\lambda_i$  may be either 0 or 1 .

We may represent this basis by a collection of binary words ( strings of 0's and 1's ) . In the usual terminology of ASF the number of 1's define the cardinality of the basis and the sequence of positions at which we have 1's  $\{S_C\}$  called the cardinality sequence labels the basis . Thus a binary sequence  $B [ C , \{ S_C \} ]$  is a representation of the member of the basis in the configuration space . The dot product between the basis members is then

$$B[C, \{S_C\}] \odot B[C', \{S_{C'}\}] = \delta_{CC'} \delta_{\{S_C S_{C'}\}}$$

A careful examination of the operations (a) - (c) defined on the configuration space , reveals that these operations change the cardinality and the cardinality sequence . Since the operations are defined on the bits of words , one can easily employ the logical functions in a computer, to define these operations .

As mentioned earlier , the symmetry considerations due to the homogeneity of disorder may be employed to reduce the rank of the effective Hamiltonian in the augmented space. The basic step in the symmetry procedure is to identify a set of nonequivalent vectors and their weights . This can be achieved in the following way . Since the augmented space is a direct product of the real space and the configuration space , which are disjoint , symmetry operations on either of them apply independently of each other . For example, if a site is occupied by an A atom , then all the  $Z$  configurations in which its  $(Z-1)$  neighbours are occupied by A atoms and one by B are equivalent . In practice a site in the augmented space is chosen as  $|R, \{C, \{S_C\}\rangle$  . All the equivalent sites are obtained by point group operation  $\mathfrak{R}$  on the site in question .

$$|R', \{C', \{S_{C'}\}\rangle = \mathfrak{R}|R, \{C, \{S_C\}\rangle = |\mathfrak{R}R, \mathfrak{R}\{C, \{S_C\}\}\rangle$$

The number of distinct sites obtained in this way is the weight of the site in question . As in the real space recursion only the non equivalent sites (NE) obtained in this way are retained for the purpose of recursion . Incorporating both the symmetry of the lattice and the orbitals, the representation of the Hamiltonian matrix element is given by :

$$\langle RL, [C, \{S_C\}] | \tilde{H} | RL, [C, \{S_C\}] \rangle = [\xi_R \tilde{C}_L + (1 - \xi_R) \tilde{C}_L] \quad (21)$$

where,

$$I \equiv |R, L [C, \{S_C\}] \rangle \in NE$$

$$\xi_R = 1 \quad R \in S_C$$

$$\xi_R = 0 \quad R \notin S_C$$

$$\tilde{C}_{RL} = x_A C^A + (1 - x_A) C^B$$

$$\hat{C}_{RL} = (1 - x_A)C^A + x_A C^B$$

The off-diagonal terms are

$$\begin{aligned} \langle R'L', [C', \{S_C\}] | \hat{H} | RL, [C, \{S_C\}] \rangle &= \sqrt{W_I/W_J} [\xi_R \xi_{R'} \bar{\Delta}^{1/2} S_{RR'} \bar{\Delta}^{1/2} + \dots \\ &+ \xi_R (1 - \xi_{R'}) \bar{\Delta}^{1/2} S_{RR'} \bar{\Delta}^{1/2} + (1 - \xi_R) \xi_{R'} \bar{\Delta}^{1/2} S_{RR'} \bar{\Delta}^{1/2} + \\ &+ (1 - \xi_R)(1 - \xi_{R'}) \bar{\Delta}^{1/2} S_{RR'} \bar{\Delta}^{1/2}] \beta_I(L, L') \delta_{[C, \{S_C\}], [C', \{S_C'\}]} \\ &\sqrt{W_I/W_J} [\xi_R \bar{\Delta}^{1/2} S_{RR'} (\delta\Delta)^{1/2} + \dots \\ &+ (1 - \xi_R) \bar{\Delta}^{1/2} S_{RR'} (\delta\Delta)^{1/2}] \beta_I(L, L') \delta_{[C, \{S_C\}], [C'+1, \{S_{C'+1}\}]} + \\ &\sqrt{W_I/W_J} [(\delta\Delta)^{1/2} S_{RR'} (\delta\Delta)^{1/2}] \dots \\ &\beta_I(L, L') \delta_{[C, \{S_C\}], [C'+2, \{S_{C'+2}\}]} \end{aligned}$$

$$\bar{\Delta}_{RL} = x_A \Delta^A + (1 - x_A) \Delta^B$$

$$\bar{\Delta}_{RL} = (1 - x_A) \Delta^A + x_A \Delta^B$$

$$\delta\Delta = \Delta^A - \Delta^B$$

The angular momenta indices are suppressed for convenience. We denote by I and J the augmented space vectors  $|R L, [C, \{S_C\}]$  and  $|R' L', [C', \{S_C'\}]$ .  $\beta_I(L, L')$  is 0 or 1 depending on whether the position I is a symmetric position with respect to the orbitals L, L' in augmented space. Once we have defined the Hamiltonian, and its operation in augmented space, the recursion method on the augmented space gives the configuration averaged Green function directly. The recursion method for the calculation of the configuration averaged Green function ( $G_{RL,RL}(z)$ ) is done as follows. We first chose the following as the starting state in our recursion

$$|\chi_i\rangle = |i \otimes L\rangle \otimes |\psi_0\rangle$$

The recursion co-efficients  $a_n$  and  $b_n$  are generated by

$$H|u_n\rangle = a_n|u_n\rangle + b_{n+1}|u_{n+1}\rangle + b_n|u_{n-1}\rangle$$

$$a_n = \langle \chi_n | \odot \hat{H} | \chi_n \rangle$$

$$b_n = \langle \chi_{n-1} | \odot \hat{H} | \chi_n \rangle$$

The continued fraction coefficients are generated to a finite numbers of steps and finally appended with a suitable terminator as discussed earlier. The configuration averaged Green function is related to the density of states by

$$n(E) = -\frac{1}{N\pi} \text{Im} \sum_L \sum_R \langle G_{RL,RL}(E + i0) \rangle \quad (22)$$

## 6 COMPUTATIONAL DETAILS.

The formalism developed in the previous section is applied to calculate the total and local density of states of random binary alloys at various concentrations. We now mention some details concerning the numerical part of the problem. Total energy density-functional calculations were performed for the elements. The Kohn-Sham equations were solved in the local density approximation (LDA) [29]. The LDA was treated within the context of the method of linear muffin tin orbitals (LMTO) in the atomic sphere approximation. The computations were performed semi-relativistically using the exchange-correlation potential of Barth and Hedin [30]. The basis set composed of  $\ell = 0, 1, 2$  orbitals, so that the Hamiltonian element are matrices of order 9. The elemental potential parameters were used to parametrize the alloy Hamiltonian, incorporating the volume derivative correction for changes with lattice parameter. The flexibility of the choice of the Wigner-Seitz radius is an advantage in the LMTO method over other muffin-tin methods like KKR. It allows to take into account the charge self-consistency approximately as emphasized by Kudrnovský *et. al.* [5]. We have adopted this scheme in our present communication

and deferred the full charge self-consistency for a later work . It is worth mentioning at this point that full charge self-consistency can easily be achieved in our formalism in the following way .

From the local density of states one can calculate the energy moments , hence the local charge density through the relation :

$$n_{RL}(r) = 1/4\pi \sum \{m_{RL}^{(0)}\phi_{RL}^2(r) + 2m_{RL}^{(1)}\phi_{RL}(r)\dot{\phi}_{RL}(r) + m_{RL}^{(2)}(\dot{\phi}_{RL}^2(r) + \phi_{RL}(r)\ddot{\phi}_{RL}(r))\} \quad (23)$$

where

$$m_{RL}^{(q)} = \int_{-\infty}^{E_F} dE n_{RL}(E)(E - E_{v,RL})^q \quad (24)$$

$n_{RL}(E)$  is the orbital projected partial density of states . From the charge density we calculate the Hartree potential by solving the Poisson equation and incorporate the exchange-correlation part by the local density functional formalism . The Schrödinger equation is then solved to obtain the potential parameters for each element in the alloy . The augmented space recursion is then carried out again with these new potential parameters , to obtain the new charge density . The procedure is iterated till self-consistency is reached . For the purpose of augmented space recursion , a four shell augmented space map was generated from a cluster of 400 sites , with interactions upto second nearest neighbour for the bcc structure and upto first nearest neighbour for the most closed packed fcc based structures . We have calculated the component and total density of states through the recursion method with 8 pairs of recursion co-efficients and terminated with the Lucini-Nex terminator [26]. In some typical cases ( CuZn to be discussed later ) , the recursion coefficients were calculated with 10 steps. For the pure elements since the density of state has considerable structure we have employed 15 steps of recursion . We have shown in our previous communication [31] that this optimum choice reproduces the density of states comparable to those obtained by other methods .

In the present communication we have studied three fcc based alloy systems : AgPd,

CuPd and Cu-rich CuZn , and two bcc based alloy systems FeTi and Zn-rich CuZn . Our results are summarised in the next section .

## 7 RESULTS AND DISCUSSION.

### 7.1 AgPd

AgPd is one of the typical alloy systems where the disorder is dominated by the diagonal part of the Hamiltonian . Both constituents have roughly the same d-band widths . Since they belong to the same row of the periodic table , they have very little mismatch in atomic sizes . The alloy remains fcc throughout the concentration regime . Further , since the effect of off-diagonal disorder is weak in this alloy system , the calculations based on CPA provide good results . Figure 1 shows the total and the component density of states for the  $Ag_x Pd_{1-x}$  random systems . We find that our density of states have the same features as that obtained by both the KKR-CPA [32] and the LMTO-CPA [5] method , with a pronounced impurity peak due to Pd for the Ag rich alloys . The general shape of the density of states of the constituents , the position of the Fermi energy and the dominant peaks agree excellently well with both the CPA calculations , in accordance to our expectation .

### 7.2 CuZn

CuZn is an important alloy system with both diagonal and off-diagonal disorder . Further ,since the centre of the Cu d band and Zn d band are well apart ,they give rise to split bands with a relatively wide band gap in between. For small concentrations of Cu or Zn one expects an impurity band splitting into bonding and anti-bonding peaks . This is a typical feature which does not show up in CPA calculations [33], and one needs to include cluster effects . This system provides a testing ground of our methodology which takes us beyond CPA .

If we carefully examine the phase diagram of  $Cu_x Zn_{1-x}$  alloy , we find that it is dominated by several ordered structures along with both fcc ( $\alpha$ ) and bcc ( $\beta$ ) solid solutions .

In our calculation we will assume fcc ( $\alpha$ ) solid solutions for  $x > 0.5$  and bcc ( $\beta$ ) solid solutions for  $x < 0.5$ . For  $x = 0.5$  one has the well-known  $\beta$ -brass, for  $x = 0$  hcp Zn and for  $x = 1.0$  fcc Cu structure. We have calculated the band energy for  $\text{Cu}_{50}\text{Zn}_{50}$  in both the fcc and bcc lattice. Our band energy calculations show the bcc phase to be more stable compared to the fcc phase.

Figure 2 shows the total and the local density of states for the  $\text{Cu}_x\text{Zn}_{1-x}$  alloy for  $x > 0.5$  where the lattice structure is taken as fcc and for  $x < 0.5$  with the alloy assumed to be in bcc phase. We find that the large difference in the d-band centre of the constituents and the difference in their widths gets reflected in the density of states. We notice that the density of states in the bcc phase has similar features as compared to that in the fcc structure.

Figure 3(a) shows the  $\text{Cu}_x\text{Zn}_{1-x}$  alloy with  $x = 0.9$ . The dotted figure is obtained by a 4-step recursion and invoking moment argument one can compare this result with the characteristic featureless CPA density of states. The solid one is obtained by a 10 step augmented space recursion. We find that in the latter, the impurity peak due to Zn gets split into bonding and antibonding peaks, because of Zn-Zn clusters in the random background. In figure 3(b) we have plotted density of states for  $\text{Cu}_x\text{Zn}_{1-x}$  alloy with  $x = 0.1$  and we observe the same cluster effects at the Cu-site.

### 7.3 CuPd

CuPd is an alloy whose constituents belong to different columns of the periodic table. As a result it has sizeable off-diagonal disorder. The mismatch between its constituents' Wigner-Seitz sphere radii leads to local distortions of the lattice. Since this is an alloy with predominant off-diagonal disorder conventional empirical TB-CPA [34] calculations give results unsatisfactory as compared to that of AgPd. In the LMTO-CPA [5] calculations the off diagonal disorder in the multiplicative factor  $\Delta$  is taken into account by mapping the Hamiltonian into an effective Hamiltonian with only diagonal disorder. However local distortions in the underlying lattice, arising out of the size mismatch between the

constituents causes disorder in the structure matrix elements  $S_{RR'}^{\alpha}$ . In general, the disorder in  $S_{RR'}^{\alpha}$  depends upon the occupation of R and R' and all their neighbouring sites. Under the *terminal point approximation*, which assumes that the major contribution comes from the occupation of the sites R and R' alone,  $S_{RR'}^{\alpha}$  has a tri-modal probability distribution with possible values  $S_{RR'}^{AA}$ ,  $S_{RR'}^{BB}$  and  $S_{RR'}^{AB}$ . This disorder is truly off-diagonal in nature, in the sense that it is not in the multiplicative form. In principle, the reduction into an effective Hamiltonian with on-site disorder is not possible. Kudrnovský and Drchal in their LMTO-CPA calculation have provided an approximate way of tackling this problem in which the entire effect of the lattice distortion has been clumped into the modification of  $\Delta$  and  $\gamma$  parameters. Since in the present methodology (ASR), the form of the Hamiltonian is kept intact with both diagonal and off-diagonal disorder, so ASR can be employed to treat lattice relaxation effect accurately at least in the terminal point approximation. We present here our calculation (figure 4(a)) for total and local density of states without lattice relaxation effect taken into account. The density of states for different concentrations with their different peak positions are in fairly good agreement with that obtained in previous works [5, 35]. It has been argued by Kudrnovský and Drchal that in case of KKR-CPA [35] use of a single muffin-tin radius for different atoms overscreens the larger atom, leading to a shift of the d-states to lower energies, but in the LMTO calculation with flexibility of the choice of the atomic sphere radii, one expects a shift of low energy peaks upwards in Cu-rich alloy compared to the KKR calculation. Our density of states clearly possesses this feature.

In figure 4(b) we present preliminary calculations of the partial density of states of Pd in  $\text{Cu}_{75}\text{Pd}_{25}$  with and without lattice relaxation. We observe the characteristic narrowing of the d-band. Such narrowing has also been seen in the approximate treatment of Kudrnovský and Drchal [5]. The details of the treatment of off-diagonal disorder due to size mismatch will be reported in a subsequent communication.

## 7.4 FeTi.

In figure 5 we present the total and local density of states for bcc FeTi alloy at various concentrations. In FeTi alloys one has disorder effect in all three elements of the Hamiltonian matrix, namely  $C^\alpha$ ,  $\Delta^\alpha$  and  $S^\alpha$ . The disorder in  $S^\alpha$  leads to lattice relaxation similar to the CuPd system. Theoretical band structure calculations for FeTi alloy are available in both LMTO-CPA [5] and KKR CPA [36] Our preliminary calculation excluding lattice relaxation effect and proper treatment of charge transfer effect shows that the results compare satisfactorily with earlier calculations, proving the applicability of the methodology to different alloy systems.

## 8 CONCLUSIONS

The calculation scheme developed in this work is based on three methodologies : (i) the TB-LMTO for the description of the hamiltonian, (ii) the Augmented Space Theorem for the configuration averaging and (iii) the recursion method on augmented space to obtain the configuration averaged Green function.

The TB-LMTO hamiltonian is free from fitted parameters. The potential parameters entering into the Hamiltonian are derived self-consistently . However, it carries with it the approximations involved in the linearization which leads to the LMTO. The recursion method requires the use of a sparse hamiltonian. We have to base our method on a less accurate Hamiltonian (which a truncation of the infinite series ( 7)) than the Hamiltonian in the so-called  $\gamma$  representation used in the CPA calculations. However, Nowak *et.al.* [16] have shown that the calculations for the density of states converge rapidly as we take more terms in the series in equation ( 7).

The configuration averaging scheme is based on the Augmented Space Theorem, which is formally exact. The use of the recursion technique with suitable terminators on the augmented space,so constructed, makes sure of the fact that the TBLMTO-ASR Green functions retain the essential herglotz analytic properties. In addition, the method can take into account cluster effects, off-diagonal effects arising due to disorder in the structure

matrix and correlated disorder [37].

The recursion method carries errors which are dependent on the finite cluster size and the nature of terminators used, both of which cause the electrons to experience a medium that deviates from the intended structures away from the central sites [15]. The choice of proper terminators partially solves the problem and one should choose larger clusters with greater number of recursion steps for more accuracy. The recursion method is a well established procedure that has proven to produce a very accurate density of states for d-bands for 8 to 15 recursion steps (that is it yields 16 to 30 moments of the density of states exactly).

In summary, we should like to propose the TB-LMTO ASR as a simple, accurate and computationally efficient method for the first-principles calculation of the electronic structure of disordered solids.

## References

- [1] Pettifor D. *Electron Theory in Alloy Design* ed. Pettifor D. and Cottrell A (London : The Institute of Materials ) p 81 (1992)
- [2] Andersen O. K. and Jepsen O. , Phys. Rev. Lett. **53** 2571 (1984)
- [3] Carr R. and Parinello M. , Phys Rev Lett **55** 2471 (1985)
- [4] Methfessel M. and Schilfgaard M. ,Int. J. Mod. Phys. **B7** 262 (1993)
- [5] Kudrnovský J. and Drchal V. , Phys. Rev. **B 41** 7515 (1990)
- [6] Kudrnovský J., Bose S.K. and Andersen O.K., Phys. Rev. **B43** 4613 (1991)
- [7] Singh P. P. and Gonis A. , Phys. Rev. **B 48** 1989 (1993)
- [8] Slater J.C., Phys. Rev. **51** 846 (1937)
- [9] Korringa J., Physica **13** 392 (1947); Kohn W. and Rostocker N., Phys. Rev. **94** 1111 (1954)
- [10] Jansen H. J. F. and Freeman A. J. , Phys Rev **B30** 561 (1984)
- [11] Andersen O.K., Phys. Rev. **B12** 3060 (1975)
- [12] See references in Stocks G.M. and Winter H., *Electronic Structure of Complex Systems* ed. P. Phariseau and W.M.Temmerman (Plenum, NY) (1985)
- [13] Kumar V., Mookerjee A. and Srivastava V.K., J. Phys. **C15** 1939 (1982)
- [14] Gonis A., Butler W.H. and Stocks G.M., Phys. Rev. Lett. **50** 1482 (1983)
- [15] Bose S.K., Kudrnovský J., Jepsen O. and Andersen O.K., Phys. Rev. **B45** 8272 (1992)
- [16] Nowak H.J., Andersen O.K., Fujiwara T., Jepsen O. and Vargas P., Phys. Rev. **B44** 3577 (1991)
- [17] Gonis A., Stocks G.M., Butler W.H. and Winter H., Phys. Rev. **B29** 555 (1984)
- [18] Tsukada M., J. Phys. Soc. Jpn. **32** 1475 (1972)
- [19] Gray L.J. and Kaplan T., J.Phys. **C9** L303, L483 (1976) ; Phys. Rev. **B14** 3462 (1976) ; Phys. Rev. **B15** 3260, 6005 (1977)
- [20] Mookerjee A., J. Phys. **C17** 1511 (1987)
- [21] Mookerjee A. , J. Phys. **C 6** 1340 (1973)
- [22] Rajput S.S., Razee S.S.A., Prasad R. and Mookerjee A., J.Phys. Condens. Matter. **2** 2653 (1990); Phys. Rev. **B42** 9391 (1990)
- [23] Haydock R. , Heine V. and Kelly M. J. , J. Phys. **C 5** 2845 (1972)
- [24] Andersen O.K.,Jepsen O., Glötzel D. in *Highlights of Condensed Matter Theory* ed. Bassani F. , Fumi F. and Tosi M.P. (North Holland, Amsterdam) 59 (1985)
- [25] Haydock H. , Ph. D. Thesis, University of Cambridge, U. K. (1972)
- [26] Lucini M. U. and Nex C. M. M. , J Phys **C 20** 3125 (1987)
- [27] Gallagher J. , Ph. D. Thesis, University of Cambridge, U. K. (1978)
- [28] Datta A. and Mookerjee A. , Int. J. Mod. Phys. **B6** 3295 (1992)
- [29] Kohn W. and Sham L. J. , Phys Rev **140A** 1133 (1965)
- [30] Von Barth U. and Hedin L. , J Phys **C5** 1629 (1972)
- [31] Saha T., Dasgupta I. and Mookerjee A., J. Phys. Condens. Matter. **L** (in press) (1994)

- [32] Winter H. and Stocks G.M., Phys. Rev. **B27** 882 (1983)
- [33] Bansil A. , Phys Rev **B10** 4096 (1979)
- [34] Laufer P. M. and Papaconstantinopoulos D. A. , Phys Rev **B35** 9019 (1987)
- [35] Winter H. , Durham P. J. , Temmerman W. M. and Stocks G. M. , Phys Rev **B23** 2370 (1986)
- [36] DaSilva E. Z. , Strange P. , Temmerman W. M. and Gyorfyy B. , Phys Rev **B36** 3015 (1987)
- [37] Razee S. S. A. and Prasad R. , Phys. Rev. **B 48** 1349,1361 (1993); Datta A. , Thakur P. K. and Mookerjee A. , Phys. Rev. **B 48** 8567 (1993) ; Mookerjee A. and Prasad R. , Phys. Rev. **B 48** 17724 (1993)

#### FIGURE CAPTIONS

**Figure 1.** The total (solid) and partial densities of states on Ag (dotted) and Pd (dashed) in  $Ag_x Pd_{1-x}$  alloys. The concentrations are from top to bottom :  $x=1, 0, 0.75, 0.5, 0.25$  and  $0$ . The vertical lines show the position of the Fermi Energy.

**Figure 2.** The total density of states for  $Cu_x Zn_{1-x}$  alloys (a) bcc with  $x=0.1$  (b) bcc with  $x=0.5$  (c) fcc with  $x=0.5$  (d) fcc with  $x=0.75$  (e) fcc with  $x=0.9$ .

**Figure 3(a).** The partial density of states at the Cu site in a bcc  $Cu_x Zn_{1-x}$  with  $x=0.1$  (dotted) CPA (full) ASF calculation with 10 steps of recursion.

**Figure 3(b).** The partial density of states at the Zn site in a fcc  $Cu_x Zn_{1-x}$  with  $x=0.9$  (dotted) CPA (full) ASF calculation with 10 steps of recursion.

**Figure 4(a).** The total (solid) and partial densities of states on Cu (dotted) and Pd (dashed) in  $Cu_x Pd_{1-x}$  alloys. The concentrations are from top to bottom :  $x=1, 0, 0.5, 0.25$  and  $0$ . The vertical lines show the position of the Fermi Energy.

**Figure 4(b).** The partial density of states at a Pd site for a  $Cu_{75}Pd_{25}$  alloy with (solid) and without (dashed) lattice relaxation.

**Figure 5.** The total (solid) and partial densities of states on Ti (dotted) and Fe (dashed) in  $Fe_x Ti_{1-x}$  alloys. The concentrations are from top to bottom :  $x=1, 0, 0.5, 0.2$  and  $0$ . The vertical lines show the position of the Fermi Energy.

#### ACKNOWLEDGEMENTS

We should like to record our thanks to Patricio Vargas for the use of his real space structure factor programme and to G.P. Das for several fruitful discussions. A.M. would like to acknowledge the Department of Science and Technology for its project SP/S2/M09/93 and the International Centre for Theoretical Physics for the Network on Metals and Alloys.

FIGURE.2

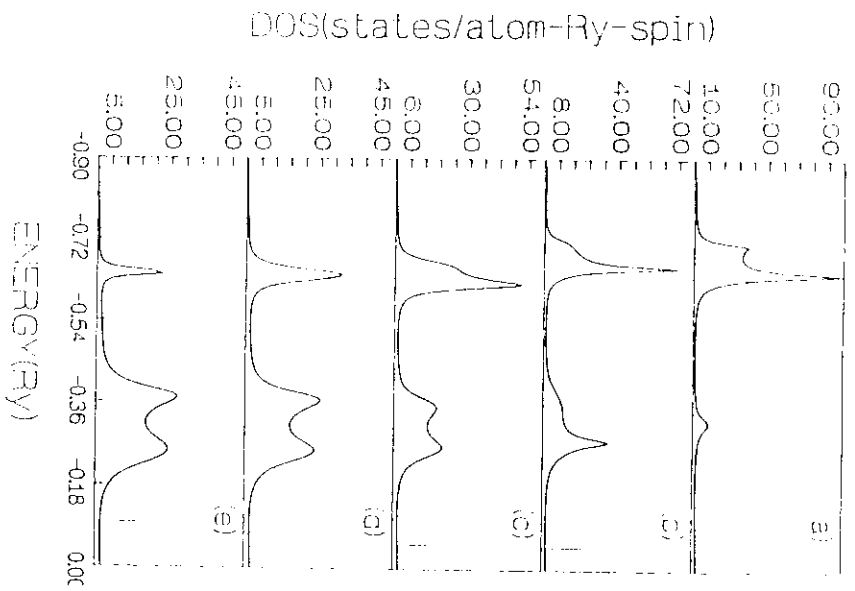


FIGURE.1

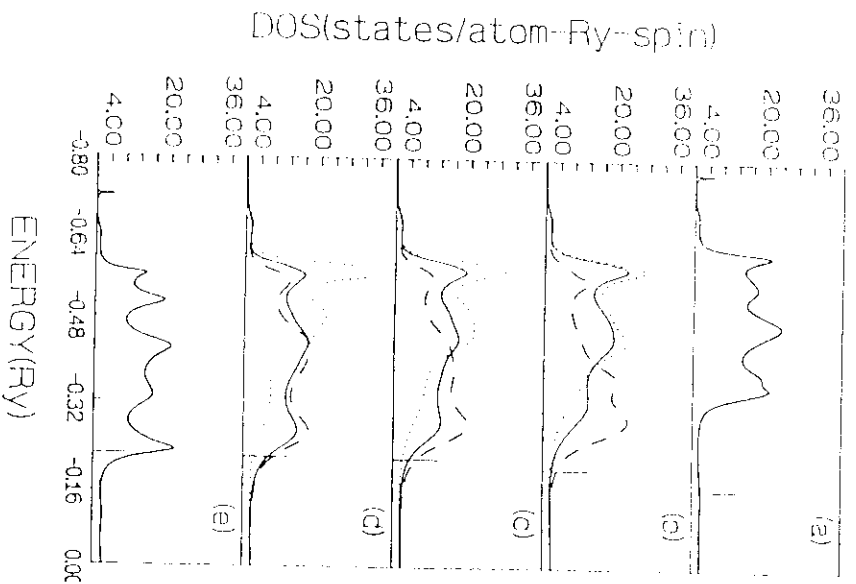


FIGURE.4(a)

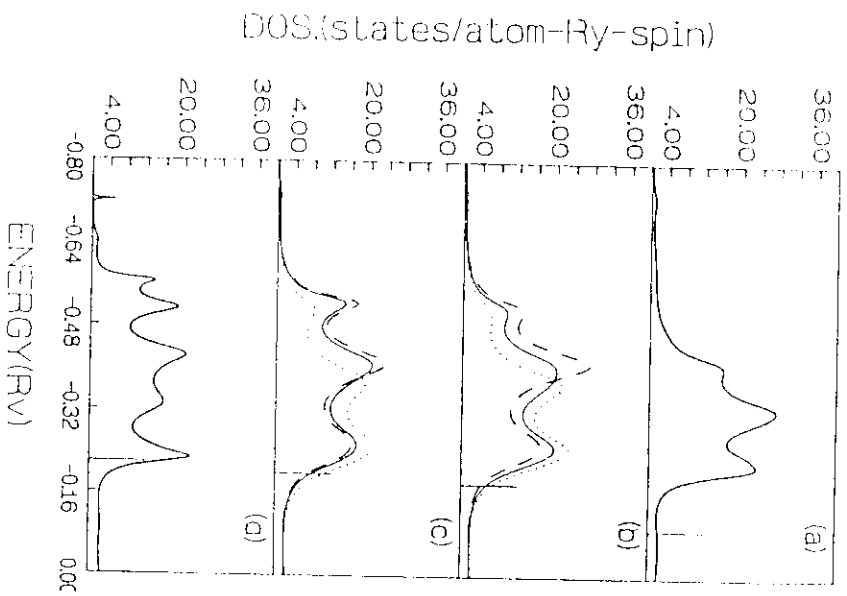


FIGURE.3(a)

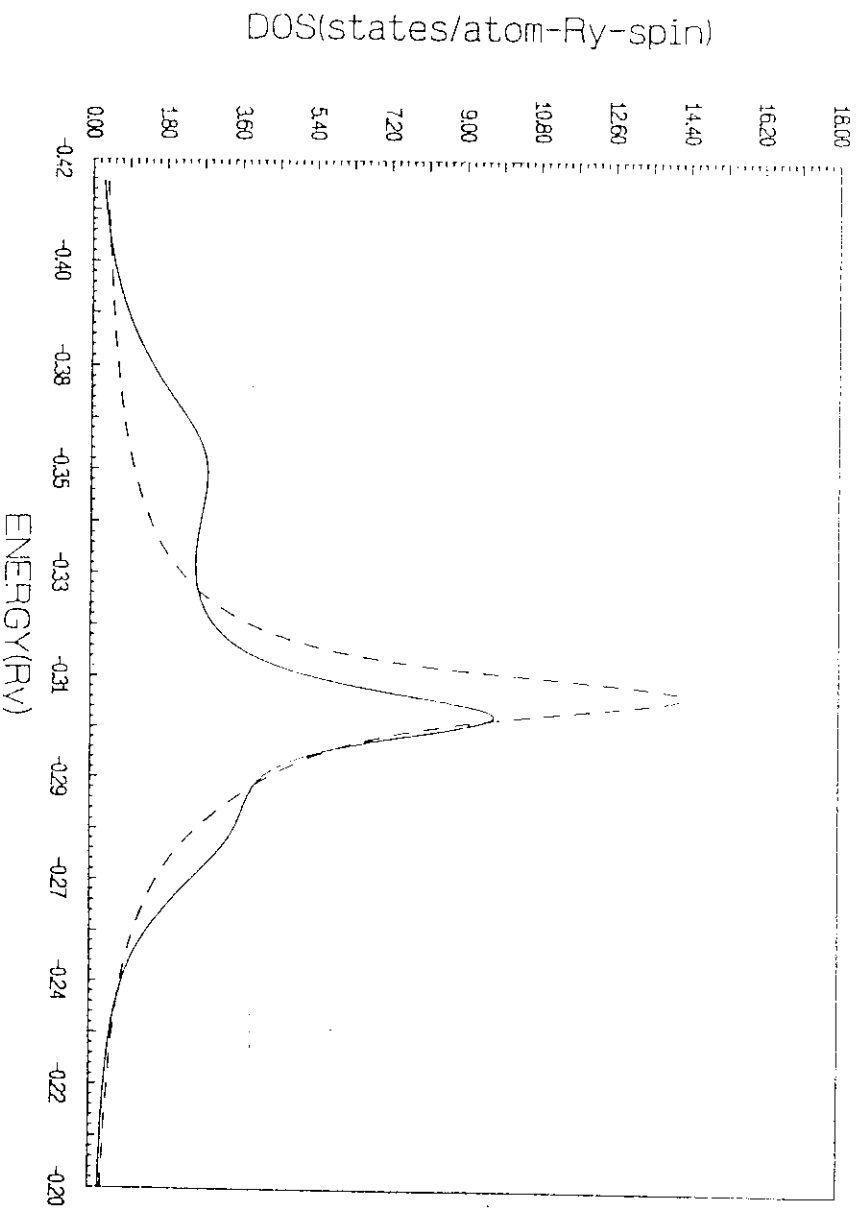


FIGURE.5

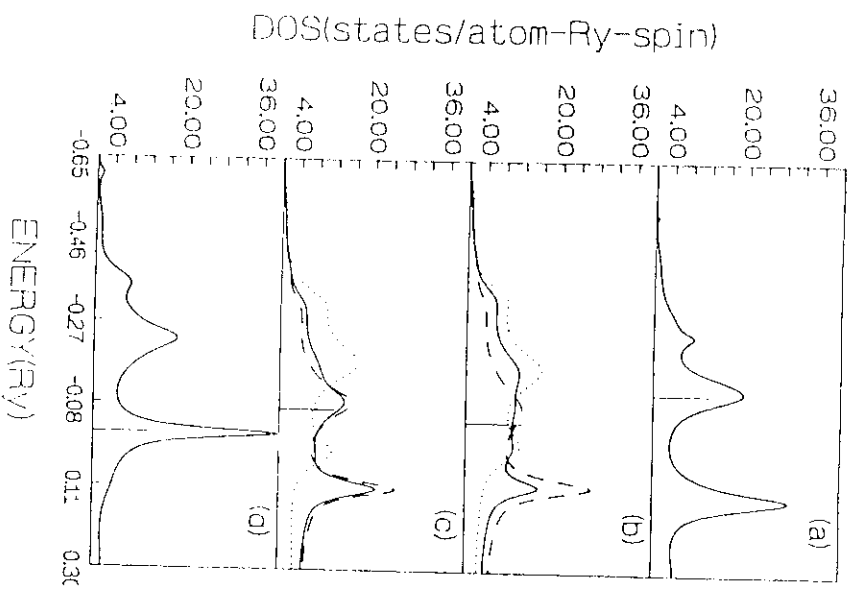


FIGURE.3(b)

